JAERI-M
86-148

CHARACTERISTICS OF PELLET AND NEUTRAL-BEAM INJECTED SINGLE NULL DIVERTOR DISCHARGES OF THE JFT-2M TOKAMAK

September 1986

Yukitoshi MIURA, Satoshi KASAI, Seio SENGOKU,
Koichi HASEGAWA, Norio SUZUKI, Mitsuru HASEGAWA[*1],
Katsumichi HOSHINO, Hisato KAWASHIMA,
Tomohide KAWAKAMI, Tohru MATOBA, Toshiaki MATSUDA,
Hiroshi MATSUMOTO, Masahiro MORI, Kazuo ODAJIMA,
Hiroaki OGAWA, Toshihide OGAWA, Hideo OHTSUKA,
Teruaki SHOJI, Susumu TAKADA[*2], Hiroshi TAMAI,
Yoshihiko UESUGI, Takumi YAMAMOTO and
Toshihiko YAMAUCHI

日本原子力研究所
Japan Atomic Energy Research Institute

JAERI-M レポートは，日本原子力研究所が不定期に公刊している研究報告書です。
入手の問合わせは，日本原子力研究所技術情報部情報資料課（〒319—11 茨城県那珂郡東海村）あて，お申しこしください。なお，このほかに財団法人原子力弘済会資料センター（〒319-11 茨城県那珂郡東海村日本原子力研究所内）で複写による実費頒布をおこなっております。

JAERI-M reports are issued irregularly.
Inquiries about availability of the reports should be addressed to Information Division, Department of Technical Information, Japan Atomic Energy Research Institute, Tokai-mura, Naka-gun, Ibaraki-ken 319-11, Japan.

© Japan Atomic Energy Research Institute, 1986

編集兼発行　日本原子力研究所
印　　刷　山田軽印刷所

JAERI-M 86-148

Characteristics of Pellet and Neutral-Beam Injected Single Null Divertor Discharges of the JFT-2M Tokamak

Yukitoshi MIURA, Satoshi KASAI, Seio SENGOKU,
Koichi HASEGAWA, Norio SUZUKI, Mitsuru HASEGAWA*1,
Katsumichi HOSHINO, Hisato KAWASHIMA, Tomohide KAWAKAMI,
Tohru MATOBA, Toshiaki MATSUDA, Hiroshi MATSUMOTO,
Masahiro MORI, Kazuo ODAJIMA, Hiroaki OGAWA,
Toshihide OGAWA, Hideo OHTSUKA, Teruaki SHOJI,
Susumu TAKADA*2, Hiroshi TAMAI, Yoshihiko UESUGI,
Takumi YAMAMOTO and Toshihiko YAMAUCHI

Department of Thermonuclear Fusion Research
Naka Fusion Research Establishment
Japan Atomic Energy Research Institute
Naka-machi, Naka-gun, Ibaraki-ken

(Received September 22, 1986)

When a single pellet is injected before the H-mode (high confinement mode) transition of neutral-beam heated single null divertor discharges, three different types of discharges are classified by the increment of line-averaged electron density ($\Delta\bar{n}_{ep}$) at the pellet injection time. One of these three types of the discharges is obtained only in the transient phase, however, the very high confinement state of the neutral-beam heated plasma is discovered. The characteristics of this type of the discharge are as follows; when $\Delta\bar{n}_{ep}$ is greater than about 4×10^{19} m^{-3}, the energy confinement time exceeds that of ohmically heated discharges and volume averaged toroidal beta, $<\beta_t>$, reaches close to the β-limit by only the neutral-beam power of 0.69MW ($<\beta_t>\sim1.6\%$ at I_p=0.22MA, a=0.25m, B_T=1.2T and $q_\psi\sim2.5$).

Keywords: Pellet, H-mode, Neutral-beam, Single Null Divertor, Confinement Time, Toroidal-beta, β-limit

---

*1 On leave from Mitsubishi Electric Co.
*2 On leave from Mitsubishi Electric Computer Systems Tokyo Co.

JFT−2Mトカマクにおけるペレット及び中性子ビームを入射したシングルヌルダイバータ放電の特徴

日本原子力研究所那珂研究所核融合研究部

三浦　幸俊・河西　敏・仙石　盛夫・長谷川浩一
鈴木　紀男・長谷川　満[*1]・星野　克道・川島　寿人
河上　知秀・的場　徹・松田　俊明・松本　宏
森　雅博・小田島和男・小川　宏明・小川　俊英
大塚　英男・荘司　昭朗・高田　晋[*2]・玉井　広史
上杉　喜彦・山本　巧・山内　俊彦

（1986年9月22日受理）

NBI加熱されたシングルヌルダイバータ放電において，高効率閉じ込めモード（H−モード）に遷移する前にペレットを入射した場合，ペレットによる密度上昇の違いにより，3種類の特徴を持つ放電に分類することができた。その中のひとつは（平均電子密度の上昇が約 4×10^{19} m^{-3} の時），時間的に変化している状態ではあるが，非常に良い閉じ込め特性を示し，エネルギー閉じ込め時間は，ジュール加熱時に得られるこのプラズマ形状での最高値を越え，60～70 msec に達する。またこの時のトロイダルベータ値は1.6％に達し，β−limit近くにあると考えられる。（$<\beta_t>$～1.6％at B_T～1.2 T，a～0.25 m，I_p～0.22 MA and q_ψ～2.5）

那珂研究所：〒311−02　茨城県那珂郡那珂町大字向山801−1

＊1　三菱電気㈱

＊2　三菱電気東部コンピュータシステム㈱

Contents

1. Introduction 1
2. Experimental Setup 1
3. Experiments and Results 2
4. Summary and Discussions 5
Acknowledgement 6
References 7

目　　次

1. 序　論 1
2. 実験装置 1
3. 実験とその結果 2
4. まとめと議論 5
謝　辞 6
参考文献 7

1. INTRODUCTION

One of the main objects of the fusion-oriented tokamak research is the production of high-β, high-confinement and high-temperature plasmas. The reason of those objects is to produce high fusion power output at low cost. Many tokamaks are devoted to the investigation of these properties of auxiliary-heated plasmas. Recently, the high confinement mode (H-mode) of neutral-beam(NB)-heated divertor discharge has been discovered first in ASDEX[1,2] and later also found in Doublet-III[3] and PDX[4]. The characteristics of the H-mode have attracted great attention since the energy confinement time of the H-mode recovers that of ohmically heated plasmas at high density region. Another high confinement mode during NB-heating has also found in ISX-B[5] (Z-mode) and in Doublet-III[6] (P-mode). In JFT-2M, the H-mode of NB-heated divertor discharge[7] or non-divertor (limiter) discharge[8] has been also discovered. The characteristics of the H-mode found in JFT-2M (hydrogen NB-heated deuterium discharge at the single null divertor configuration) are almost always the burst-free H-mode[9]. In addition to the H-mode, much higher confinement discharge has been discovered in JFT-2M. This discharge is achieved by injecting a large pellet before H-transition of NB-heated single null divertor plasma. The global energy confinement time ($\tau_E{}^G$) of this discharge exceeds that of ohmically heated ones and the volume-averaged toroidal beta ($<\beta_t>$) reaches close to the β-limit. This higher confinement mode, which is similar to divertor P-mode in D-III[6], is called "Ultra H-mode". The characteristics of a single pellet injected and NB heated discharges are reported in this paper.

2. EXPERIMENTAL SETUP

JFT-2M[10,11] is a Tokamak with D-shaped vacuum vessel (1.31m major radius and 0.415×0.595m minor radius). The maximum toroidal magnetic field (B_T) is 1.42T and the maximum Plasma current (I_p) is 0.5MA at D-shape configuration. The divertor of the JFT-2M is a simple open divertor. The material of divertor plates and limiter is carbon graphite. Figure 1 shows the top view of the JFT-2M and various diagnostic apparatus. The hydrogen NB-injection system consists of two beam lines, one of them is a Co-injection line (Co-NB), and the

1. INTRODUCTION

One of the main objects of the fusion-oriented tokamak research is the production of high-β, high-confinement and high-temperature plasmas. The reason of those objects is to produce high fusion power output at low cost. Many tokamaks are devoted to the investigation of these properties of auxiliary-heated plasmas. Recently, the high confinement mode (H-mode) of neutral-beam(NB)-heated divertor discharge has been discovered first in ASDEX[1,2] and later also found in Doublet-III[3] and PDX[4]. The characteristics of the H-mode have attracted great attention since the energy confinement time of the H-mode recovers that of ohmically heated plasmas at high density region. Another high confinement mode during NB-heating has also found in ISX-B[5] (Z-mode) and in Doublet-III[6] (P-mode). In JFT-2M, the H-mode of NB-heated divertor discharge[7] or non-divertor (limiter) discharge[8] has been also discovered. The characteristics of the H-mode found in JFT-2M (hydrogen NB-heated deuterium discharge at the single null divertor configuration) are almost always the burst-free H-mode[9]. In addition to the H-mode, much higher confinement discharge has been discovered in JFT-2M. This discharge is achieved by injecting a large pellet before H-transition of NB-heated single null divertor plasma. The global energy confinement time ($\tau_E{}^G$) of this discharge exceeds that of ohmically heated ones and the volume-averaged toroidal beta ($<\beta_t>$) reaches close to the β-limit. This higher confinement mode, which is similar to divertor P-mode in D-III[6], is called "Ultra H-mode". The characteristics of a single pellet injected and NB heated discharges are reported in this paper.

2. EXPERIMENTAL SETUP

JFT-2M[10,11] is a Tokamak with D-shaped vacuum vessel (1.31m major radius and 0.415×0.595m minor radius). The maximum toroidal magnetic field (B_T) is 1.42T and the maximum Plasma current (I_p) is 0.5MA at D-shape configuration. The divertor of the JFT-2M is a simple open divertor. The material of divertor plates and limiter is carbon graphite. Figure 1 shows the top view of the JFT-2M and various diagnostic apparatus. The hydrogen NB-injection system consists of two beam lines, one of them is a Co-injection line (Co-NB), and the

other is a Counter-injection line with respect to the direction of the plasma current. Injection angle is about 38 degrees to the major radius. The pellet injector[12] is the Oak Ridge National Laboratory (ORNL) type[13] of gas-propellant single pellet injector. The size of the pellet (design value) is $1.65mm^{\phi} \times 1.65mm^{L}$ and the reproducible speed of the pellet is about 0.7km/sec. The block diagram of the pellet injector and the ablation monitor constructed by the single and the array of photo-diode with H_α/D_α filter is shown in Fig. 2.

3. EXPERIMENTS AND RESULTS

Experiments were performed by injecting a deuterium pellet before H-transition (0.66sec in Figs. 4, 5 and 9). The injection speed of the pellet was about 0.7km/sec. The hydrogen Co-NB of 34keV was injected into the single null divertor plasmas (deuterium) from 0.65sec (time interval of the dotted vertical line in Figs. 4, 5 and 9), and heating power injected from the port was about 0.77MW (net heating power by the calculation of NBI power deposition code was about 0.69MW). Figure 3 shows the outer magnetic surface, which is closed surface of about 5mm inner from the separatrix surface, null point and various configuration parameters determined by the magnetic fitting method[11,14,15] (except B_T). Three different types of discharges are classified under these conditions. The various plasma parameters of these three types of discharges are shown in Figs. 4, 5 and 9. Two remarkable differences are found in these figures. One is the increment of the line-averaged electron density ($\bar{n}_e$) at the pellet injection time (depending on the size of a pellet), and the other is seen in the outside Mirnov loop ($\dot{\tilde{B}}_\theta$) signal.

3.1 The characteristics of the type 1 discharge (Fig. 4)

The increment of $\bar{n}_e$ at the pellet injection time [($\Delta\bar{n}_{ep}$) measured by the HCN laser interferometer shown in Fig. 4(a)] is about 1.5×10^{19} m^{-3}, and after this time the density is increasing linearly with time. The D_α-intensity [see Fig. 4(e)] apart from the singular point (near the limiter or the location of the gas puffing) decreases after the pellet injection. The bolometer signal [see Fig. 4(f)] which shows the sum of radiation and charge exchange loss power from lower half of the plasma is increasing linearly up to the time of sudden increase of

other is a Counter-injection line with respect to the direction of the plasma current. Injection angle is about 38 degrees to the major radius. The pellet injector[12] is the Oak Ridge National Laboratory (ORNL) type[13] of gas-propellant single pellet injector. The size of the pellet (design value) is $1.65mm^{\phi} \times 1.65mm^{L}$ and the reproducible speed of the pellet is about 0.7km/sec. The block diagram of the pellet injector and the ablation monitor constructed by the single and the array of photo-diode with H_α/D_α filter is shown in Fig. 2.

3. EXPERIMENTS AND RESULTS

Experiments were performed by injecting a deuterium pellet before H-transition (0.66sec in Figs. 4, 5 and 9). The injection speed of the pellet was about 0.7km/sec. The hydrogen Co-NB of 34keV was injected into the single null divertor plasmas (deuterium) from 0.65sec (time interval of the dotted vertical line in Figs. 4, 5 and 9), and heating power injected from the port was about 0.77MW (net heating power by the calculation of NBI power deposition code was about 0.69MW). Figure 3 shows the outer magnetic surface, which is closed surface of about 5mm inner from the separatrix surface, null point and various configuration parameters determined by the magnetic fitting method[11,14,15] (except B_T). Three different types of discharges are classified under these conditions. The various plasma parameters of these three types of discharges are shown in Figs. 4, 5 and 9. Two remarkable differences are found in these figures. One is the increment of the line-averaged electron density ($\bar{n}_e$) at the pellet injection time (depending on the size of a pellet), and the other is seen in the outside Mirnov loop ($\dot{B}_\theta$) signal.

3.1 The characteristics of the type 1 discharge (Fig. 4)

The increment of $\bar{n}_e$ at the pellet injection time [($\Delta\bar{n}_{ep}$) measured by the HCN laser interferometer shown in Fig. 4(a)] is about 1.5×10^{19} m^{-3}, and after this time the density is increasing linearly with time. The D_α-intensity [see Fig. 4(e)] apart from the singular point (near the limiter or the location of the gas puffing) decreases after the pellet injection. The bolometer signal [see Fig. 4(f)] which shows the sum of radiation and charge exchange loss power from lower half of the plasma is increasing linearly up to the time of sudden increase of

D_α-intensity. The global energy confinement time [$\tau_E^G = W_s/(P_{total} - dW_s/dt)$, where the stored energy (W_s) shown in Fig. 4(b) is determined from the magnetic fitting method assuming the constant internal inductance (l_i) of 1.04 and P_{total} is the total input power] of this case is shown in Fig. 4(d). After the pellet injection τ_E^G is equal to the value of ohmically heated discharges at the same density region, but decreases gradually as increasing the density and the radiation loss power. These are clearly shown by closed triangles and open squares in Fig. 8 (closed triangles show τ_E^G of this type of discharges and open squares show those of ohmically heated ones). This degradation of τ_E^G compared with that of ohmically heated discharges at the same density region may be due to the increase of the radiation loss power from the central part of the plasma. These properties shown in Fig. 4 are almost the same as the H-mode[7,9] achieved by the gas puffing operation. It is concluded that when an injected pellet is small ($\Delta\bar{n}_{ep} \leqq 2\times10^{19}m^{-3}$) the characteristics of the discharge are the same as the H-mode achieved by the gas puffing operation.

3.2 The characteristics of the type 2 discharge (Fig. 5)

This is the Ultra H-mode discharge. $\Delta\bar{n}_{ep}$ shown in Fig. 5(a) is about $4.5\times10^{19}m^{-3}$. Figure 6(a) shows the ablation profile of this large pellet measured horizontally by the single H_α/D_α detector. An ablation rate at the point of X=0.1725m, X=0.1212m, X=0.0729m and X=0.0242m can be also estimated from the signals in Figs. 6(b), 6(c), 6(d) and 6(e) respectively. These are obtained from the measurement of D_α-intensity in the vertical direction by using H_α/D_α detector array[16]. X is the length from the center of the vacuum vessel (R=1.31m) on the mid-plane. The speed of a pellet in the plasma is estimated from the peak time of the intensity and the point X in Figs. 6(b), 6(c), 6(d) and 6(e). The X-axis shown in Fig. 6(a) is converted from time to R(m) by using the estimated speed of a pellet in the plasma and points X. These signals show that the pellet is ablating mainly around r(minor radius)=0.1m and passing through the center of the outer magnetic surface. W_s shown in Fig. 3(b) is increasing linearly to the value of 34kJ. When W_s reaches 34kJ, $\dot{\hat{B}}_\theta$ signal always grows and the burst-out of the plasma energy occurs. The frequency of the $\dot{\hat{B}}_\theta$ is about 5kHz, and the growing of the $\dot{\hat{B}}_\theta$ signal occurs at the safety factor (q_ψ) of the

outer magnetic surface shown in Fig. 3 close to 2.5 (q_ψ changes from 2.9 to 2.5 during NB-heating). At this time $<\beta_t>$ is about 1.6%, and the factor of g in the equation of $<\beta_t>=g*I_p/(a*B_T)$ is about 2.2. It is considered that this results agree with the range of theoretical limits due to kink and ideal ballooning modes[17] with free boundary. Therefore, this burst-out of the plasma energy is considered to be caused by the β-limit. During increasing phase of W_s, about 70% of net NB-heated power is stored in the plasma [dW_s/dt is shown in Fig. 5(c)]. The value of 70% is the factor of 2 greater than that reported in Ref. 9. The increment of W_s is mainly due to the increment of both electron and ion temperature. Figure 7 shows the central electron and ion temperature obtained by the soft X-ray and mass-separated neutral particle measurements. Both electrons and ions are cooled down by injecting a large pellet. After injection both electron and ion temperatures are approximately equal and heated to about 0.8keV. The increasing rate and the value of W_s is roughly consistent to the measured electron and ion temperatures assuming parabolic temperature profile. The radiation loss power shown in Fig. 5(f) indicates that impurity accumulation into a plasma core is very little in this case compared with that in the H-mode. The radiation loss power and D_α-intensity do not increase up to the time of the saturation of W_s. τ_E^G shown in Fig. 5(d) increases to 60∿70msec and sustains this level for about 20msec. τ_E^G of this type of discharges shown by closed circles in Fig. 8 exceeds that of ohmically heated ones at the same density region. Three remarkable characteristics of the Ultra H-mode are concluded as follows. First, the energy confinement time of Ultra H-mode exceeds that in the ohmically heated discharge at the same density region. Second, $<\beta_t>$ reaches close to the β-limit by the NB-power of only 0.69MW. Third, the radiation loss power compared with that of the H-mode is very little.

3.3 The characteristics of the type 3 discharge (Fig. 9)

In this discharge, a large pellet is also injected, but Ultra H-mode terminates at $\dot{B}_\theta$ signal growing and discharge turns to the H-mode. $\Delta\bar{n}_{ep}$ shown in Fig. 7(a) is about $4\times10^{19}m^{-3}$. Figure 10 shows the ablation profile of this case. The ablation profile and $\Delta\bar{n}_{ep}$ are similar to the type 2 discharges. W_s is linearly increasing up to the

time of $\dot{\tilde{B}}_\theta$ signal growing [see Fig. 7(b)]. After that time W_s saturates, D_α-intensity repeats increase and decrease [see Fig. 7(e)] and radiation loss power increases with time [see Fig. 7(f)]. During the increasing phase of W_s, dW_s/dt equals to that of the discharge of type 2 [see Fig. 7(c) and 3(c)]. After the injection of a pellet, $\tau_E{}^G$ starts increase from about 35msec to 60∿70msec, but after the time of growing $\dot{\tilde{B}}_\theta$ signal, $\tau_E{}^G$ decreases to about 35msec [see Fig. 7(d)]. During increasing phase of W_s the properties of this discharge are the same as the Ultra H-mode. But after $\dot{\tilde{B}}_\theta$ signal growing Ultra H-mode terminates and the discharge shows the same properties of the H-mode. In this case, the characteristics of the discharge are concluded that the Ultra H-mode terminates when $<\beta_t>$ reaches close to the β-limit softly, and the discharge turns to the H-mode.

4. SUMMARY AND DISCUSSIONS

When a single pellet is injected before the H-mode transition of neutral-beam heated single null divertor discharges, three different types of discharges are classified by $\Delta\bar{n}_{ep}$. First, when $\Delta\bar{n}_{ep}$ is about $2\times10^{19}m^{-3}$, the discharge shows the same properties of the H-mode achieved by the gas puffing operation. Second, when $\Delta\bar{n}_{ep}$ is greater than about $4\times10^{19}m^{-3}$, the discharge shows the very high confinement state (Ultra H-mode). This discharge can be obtained only in the transient phase and temperature is only below one keV, however, $\tau_E{}^G$ exceeds that of ohmically heated ones at high density and $<\beta_t>$ reaches close to the β-limit. Third, although $\Delta\bar{n}_{ep}$ is about $4\times10^{19}m^{-3}$, when $\dot{\tilde{B}}_\theta$ signal grows before W_s reaching 34kJ the Ultra H-mode terminates to the H-mode.

Considering the linear relation between the peak value of $\tau_E{}^G$ in the Ultra H-mode discharges and $\bar{n}_e$, neoclassical ion thermal diffusivity[18] ($\chi_i{}^{neo}$) may be one of the possible explanation of this high confinement state. This is similar consideration of the high confinement state in a pellet injected ohmically heated plasmas reported in Ref. 19.

time of $\dot{B}_\theta$ signal growing [see Fig. 7(b)]. After that time W_s saturates, D_α-intensity repeats increase and decrease [see Fig. 7(e)] and radiation loss power increases with time [see Fig. 7(f)]. During the increasing phase of W_s, dW_s/dt equals to that of the discharge of type 2 [see Fig. 7(c) and 3(c)]. After the injection of a pellet, τ_E^G starts increase from about 35msec to 60∿70msec, but after the time of growing $\dot{B}_\theta$ signal, τ_E^G decreases to about 35msec [see Fig. 7(d)]. During increasing phase of W_s the properties of this discharge are the same as the Ultra H-mode. But after $\dot{B}_\theta$ signal growing Ultra H-mode terminates and the discharge shows the same properties of the H-mode. In this case, the characteristics of the discharge are concluded that the Ultra H-mode terminates when $<\beta_t>$ reaches close to the β-limit softly, and the discharge turns to the H-mode.

4. SUMMARY AND DISCUSSIONS

When a single pellet is injected before the H-mode transition of neutral-beam heated single null divertor discharges, three different types of discharges are classified by $\Delta\bar{n}_{ep}$. First, when $\Delta\bar{n}_{ep}$ is about $2\times10^{19}m^{-3}$, the discharge shows the same properties of the H-mode achieved by the gas puffing operation. Second, when $\Delta\bar{n}_{ep}$ is greater than about $4\times10^{19}m^{-3}$, the discharge shows the very high confinement state (Ultra H-mode). This discharge can be obtained only in the transient phase and temperature is only below one keV, however, τ_E^G exceeds that of ohmically heated ones at high density and $<\beta_t>$ reaches close to the β-limit. Third, although $\Delta\bar{n}_{ep}$ is about $4\times10^{19}m^{-3}$, when $\dot{B}_\theta$ signal grows before W_s reaching 34kJ the Ultra H-mode terminates to the H-mode.

Considering the linear relation between the peak value of τ_E^G in the Ultra H-mode discharges and $\bar{n}_e$, neoclassical ion thermal diffusivity[18] (χ_i^{neo}) may be one of the possible explanation of this high confinement state. This is similar consideration of the high confinement state in a pellet injected ohmically heated plasmas reported in Ref. 19.

ACKNOWLEDGEMENTS

The authors are very grateful to Drs. S. Mori, K. Tomabechi, M. Tanaka, A. Funahashi and Y. Tanaka for their continuous support of our work, and it is our pleasure to acknowledge the fine support of the JFT-2M operational group under Messrs. K. Suzuki, Y. Matsuzaki and T. Tani and neutral-beam-injection group under Mr. T. Shibata. Discussions with Dr. T. Hirayama by using 1-D Tokamak-code and with the theory group under Dr. T. Takeda are greatly acknowledged.

REFERENCES

1. F. Wagner, et al., Phys. Rev. Lett. 49, 1408 (1982).
2. F. Wagner, et al., in Proceedings of the Ninth International Conference on Plasma Physics and Controlled Nuclear Fusion Research, Baltimore, 1982 (International Atomic Energy Agency, Vienna, 1982), Vol.1, P.43.
3. M. Nagami, et al., Nucl. Fusion 24, 183 (1984).
4. S.M. Kaye, et al., in Proceedings of the Eleventh European Conference on Controlled Fusion and Plasma Physics, Aachen, 1983, Part I, P.19.
5. M. Murakami, et al., in Proceedings of the Tenth International Conference on Plasma Physics and Controlled Nuclear Fusion Research, London, 1984 (International Atomic Energy Agency, Vienna, 1985), Vol.1, P.87.
6. S. Sengoku, et al., in Proceedings of the Tenth International Conference on Plasma Physics and Controlled Nuclear Fusion Research, London, 1984 (International Atomic Energy Agency, Vienna, 1985), Vol.1, P.405.
7. S. Sengoku, et al., "Confinement and Fueling Studies during Additional Heating Phase in JFT-2M Tokamak", presented at Seventh International Conference on Plasma-Surface Interactions in Controlled Fusion Devices, (Princeton, 1986), to be appear in J. Nucl. Mater.
8. JFT-2M team, paper in preparation.
9. M. Keilhacker, et al., in Proceedings of the Tenth International Conference on Plasma Physics and Controlled Nuclear Fusion Research, London, 1984 (International Atomic Energy Agency, Vienna, 1985), Vol.1, P.71.
10. T. Shoji, et al., Japan Atomic Energy Research Institute Report No. JAERI-M 83-194, (1983) (in Japanese).
11. M. Mori, et al., submitted to Nucl. Fusion.
12. S. Kasai, et al., Japan Atomic Energy Research Institute Report No. JAERI-M 86-109, (1986).
13. S.L. Milora, et al., Rev. Sci. Instrum. 50, 482 (1979).
14. I. Yanagisawa, et al., to be published in Proceedings of Eleventh Symposium on Fusion Engineering, Austin, Texas, November 18-22, 1985.

15. D.W. Swain, et al., Nucl. Fusion 22, 1015 (1982).
16. Y. Miura, et al., Japan Atomic Energy Research Institute Report No. JAERI-M 85-192, (1985) (in Japanese).
17. F. Troyon, et al., in Proceedings of the Eleventh European Conference on Controlled Fusion and Plasma Physics, Aachen, 1983, 26, 209 (1984).
18. F.L. Hinton, et al., Rev. Mod. Phys. 48, 239 (1976).
19. M. Greenwald, et al., in Proceedings of the Tenth International Conference on Plasma Physics and Controlled Nuclear Fusion Research, London, 1984 (International Atomic Energy Agency, Vienna, 1985), Vol.1, P.45.

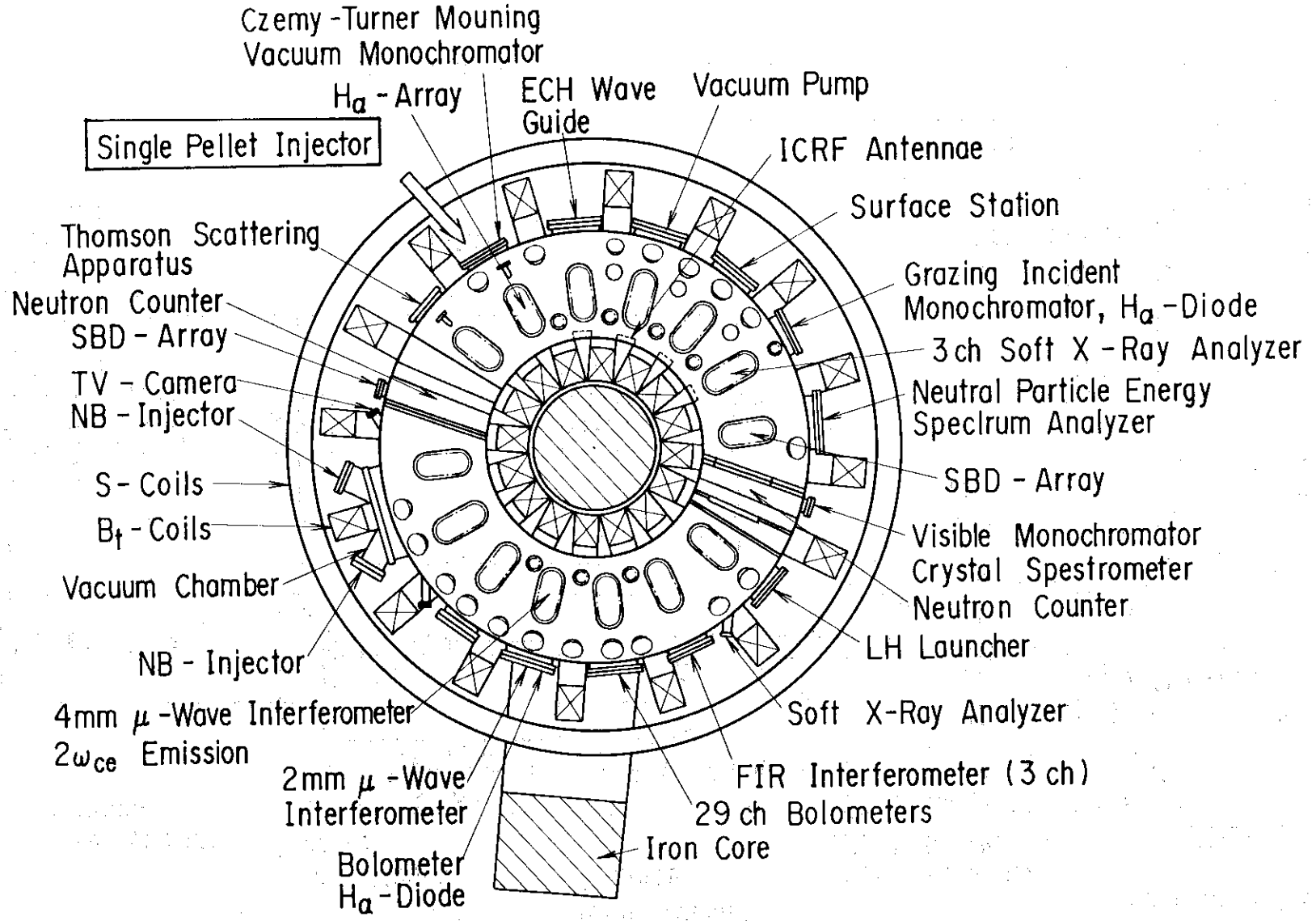

JFT-2M Tokamak and Diagnostic Apparatuses

Fig. 1 The top view of the JFT-2M and various plasma diagnostic apparatus.

JAERI-M 86-148

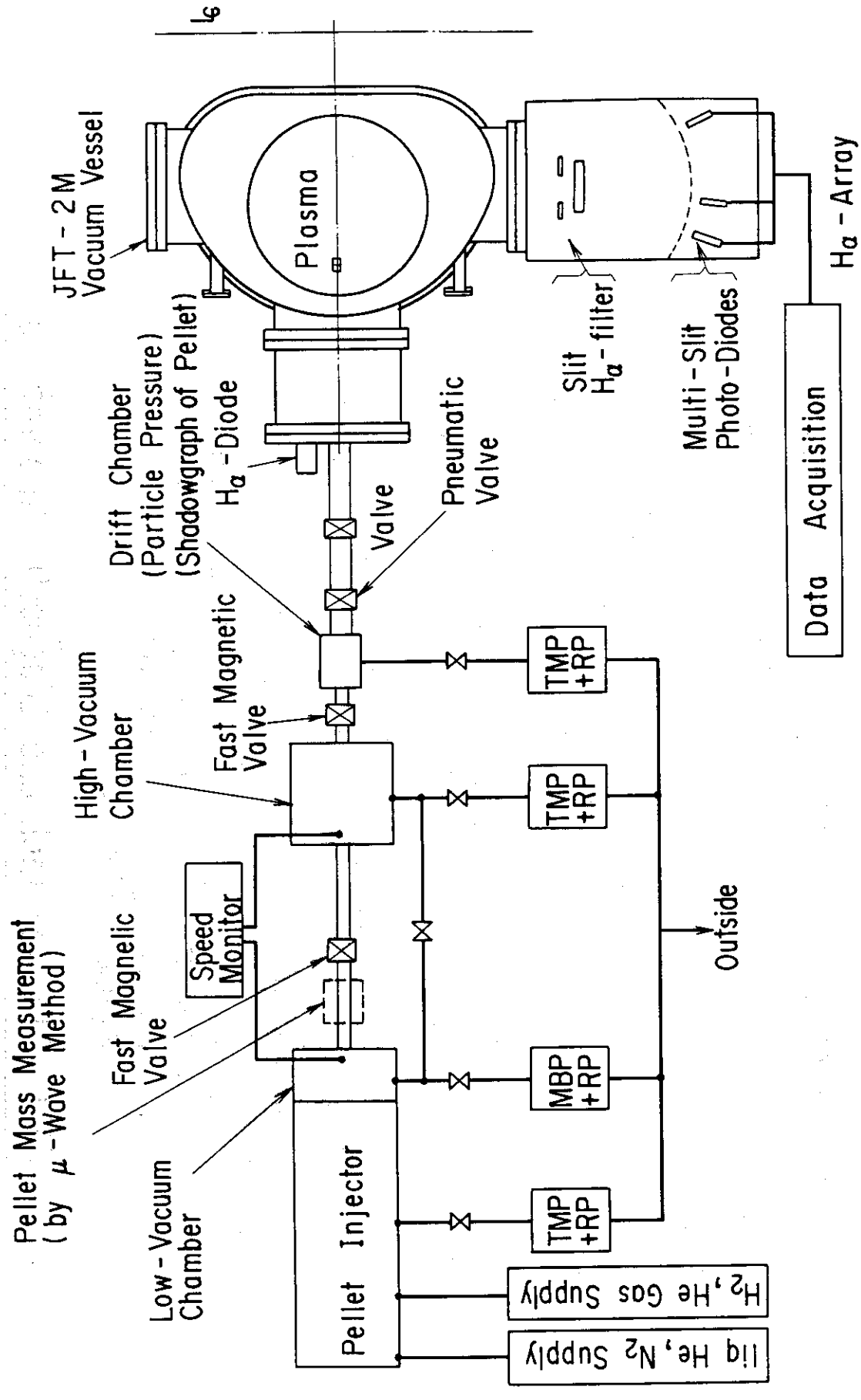

Fig. 2 The block diagram of the pellet injector and the ablation minotor system.

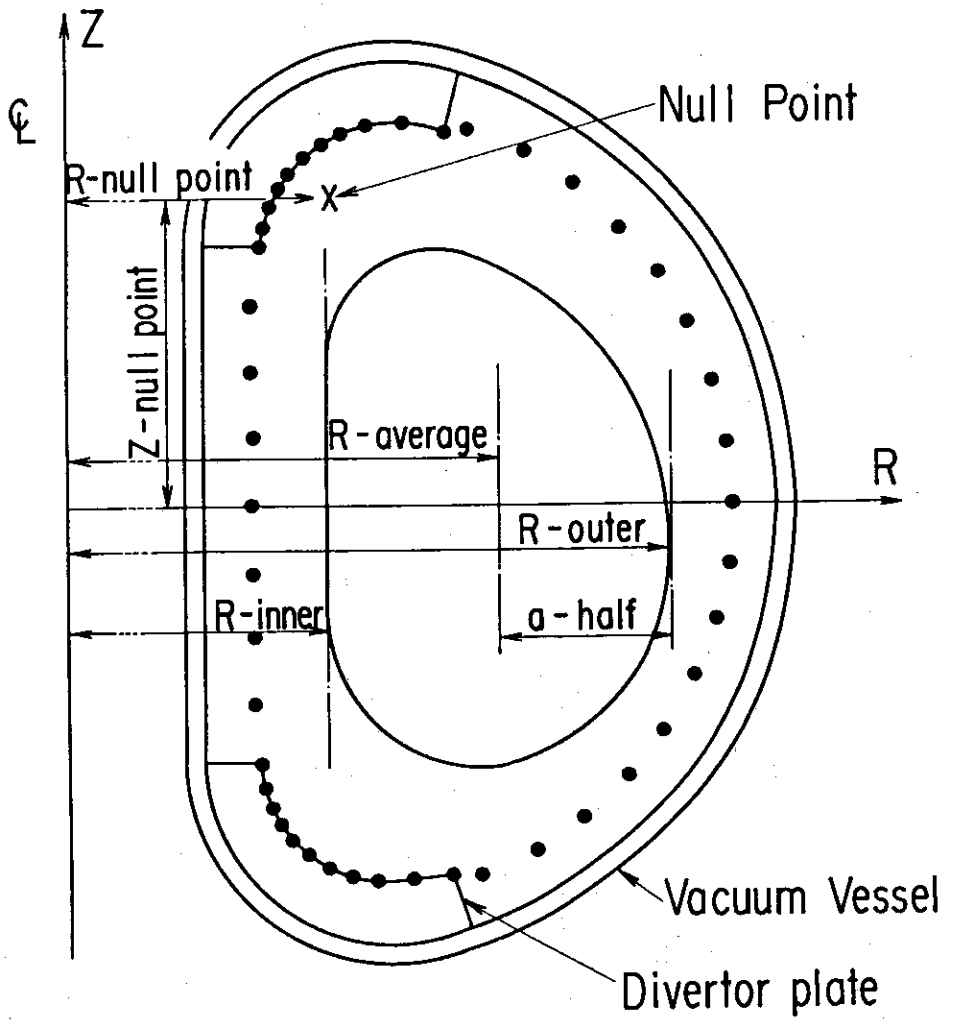

Current (I_p)	0.221	(MA)
R-average	1.318	(m)
Z-average	-0.006	(m)
R-inner	1.069	(m)
R-outer	1.565	(m)
a-half	0.249	(m)
a-average	0.298	(m)
Ellipticity	1.414	
Triangularity	0.272	
Cross Area	0.280	(m^2)
Volume	2.316	(m^3)
R-null point	1.08	(m)
Z-null point	0.41	(m)
B_T	1.20	(T)

Fig. 3 The cross section of JFT-2M vacuum vessel and outer magnetic surface, null point and various plasma parameters determined by the magnetic fitting method.
● shows the position of fixed limiter or divertor plate.

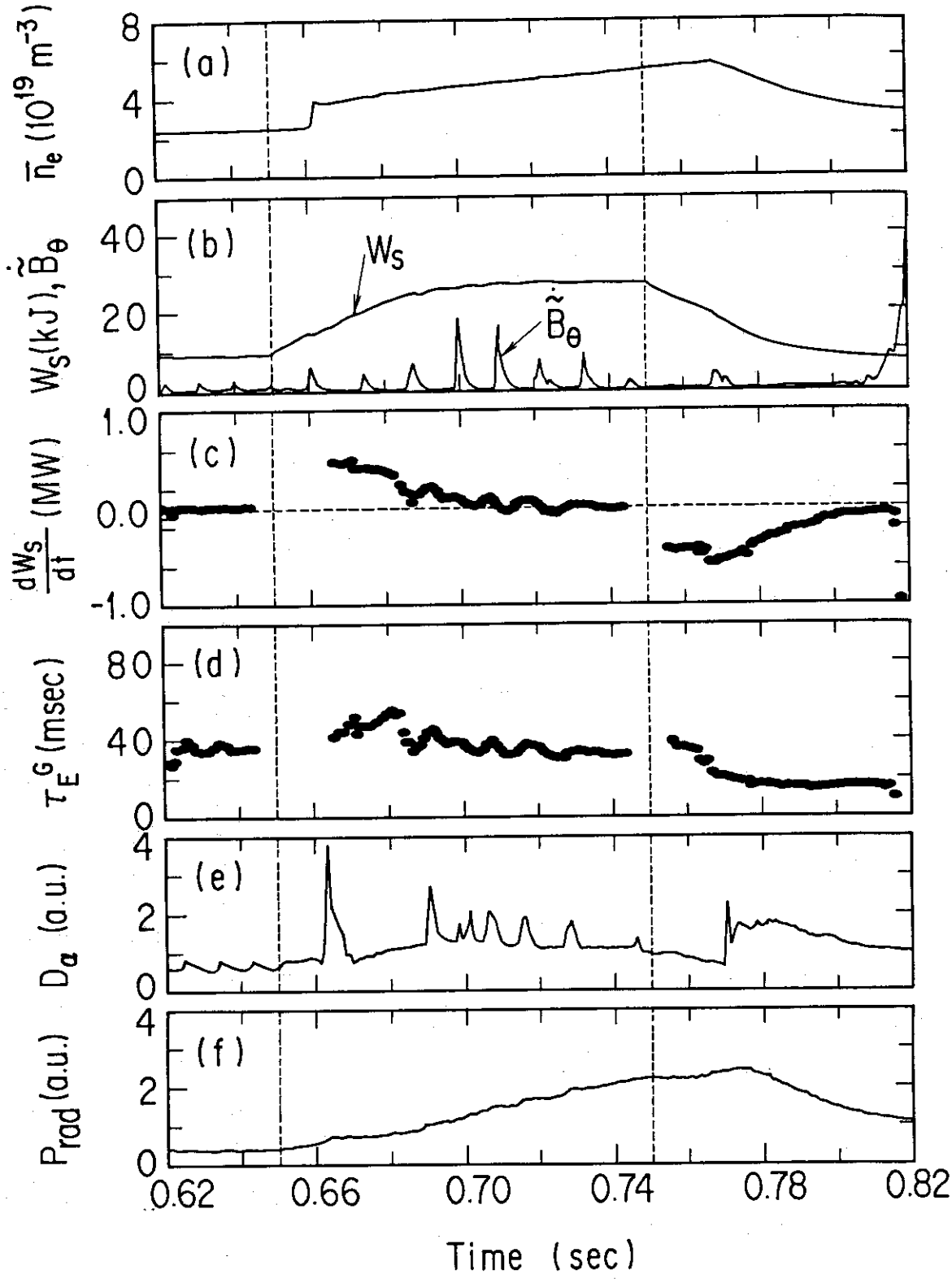

Fig. 4 Time evolution of various plasma parameters of type 1: (a) line-averaged electron density ($\bar{n}_e$), (b) stored energy (W_S) and half envelope of $\tilde{B}_\theta$ signal, (c) differential of W_S determined by fitting 5 points (5 msec) of W_S to cubic function, (d) global energy confinement time (τ_E^G), (e) D_α-intensity apart from the singular point, (f) sum of radiation and charge exchange loss power from lower half of plasma measured by the bolometer.

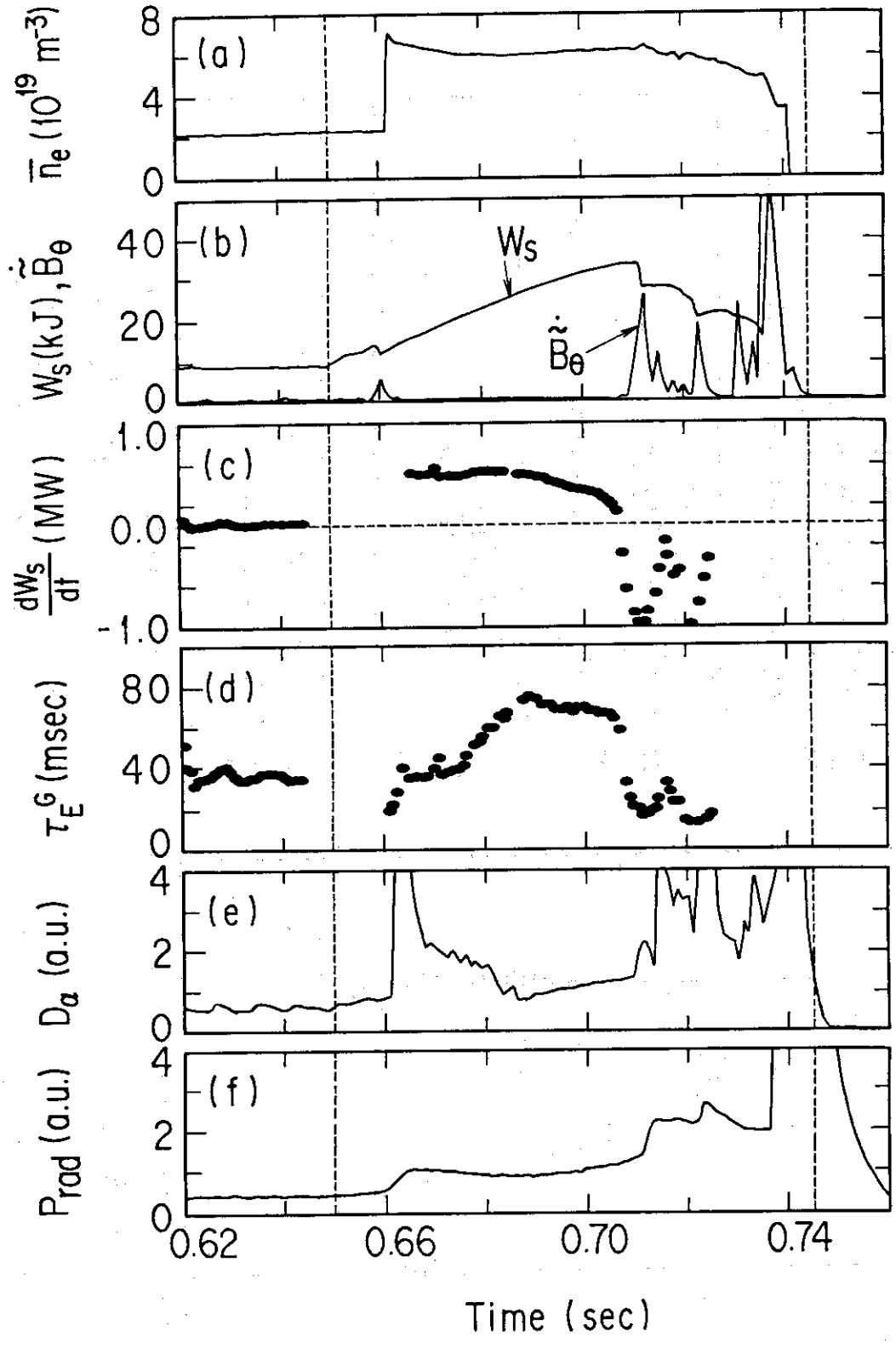

Fig. 5 Time evolution of various plasma parameters of type 2: columns from (a) to (f) are the same as Fig. 4(a) to Fig. 4(f), respectively.

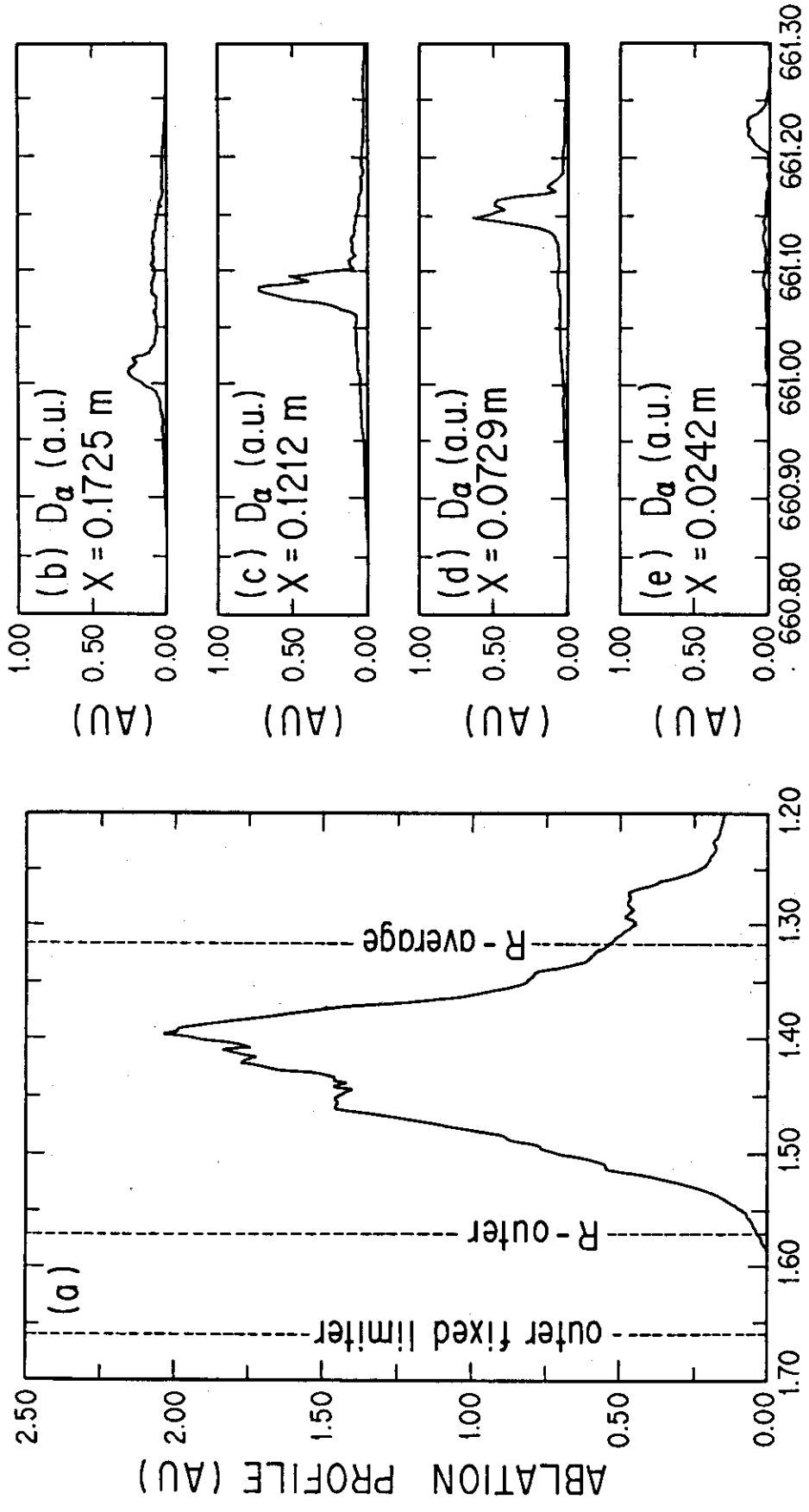

Fig. 6 Ablation profiles of the pellet of type 2 discharge: (a) ablation profile measured horizontally by a single H_α/D_α detector, (b), (c), (d) and (e) are measured vertically by H_α/D_α detector array. X in (b), (c), (d) and (e) are the length from the center of the vacuum vessel (R=1.31m) on the mid-plane. The positions of fixed-limiter (on the mid-plane), R-outer and R-average correspond to Fig. 3.

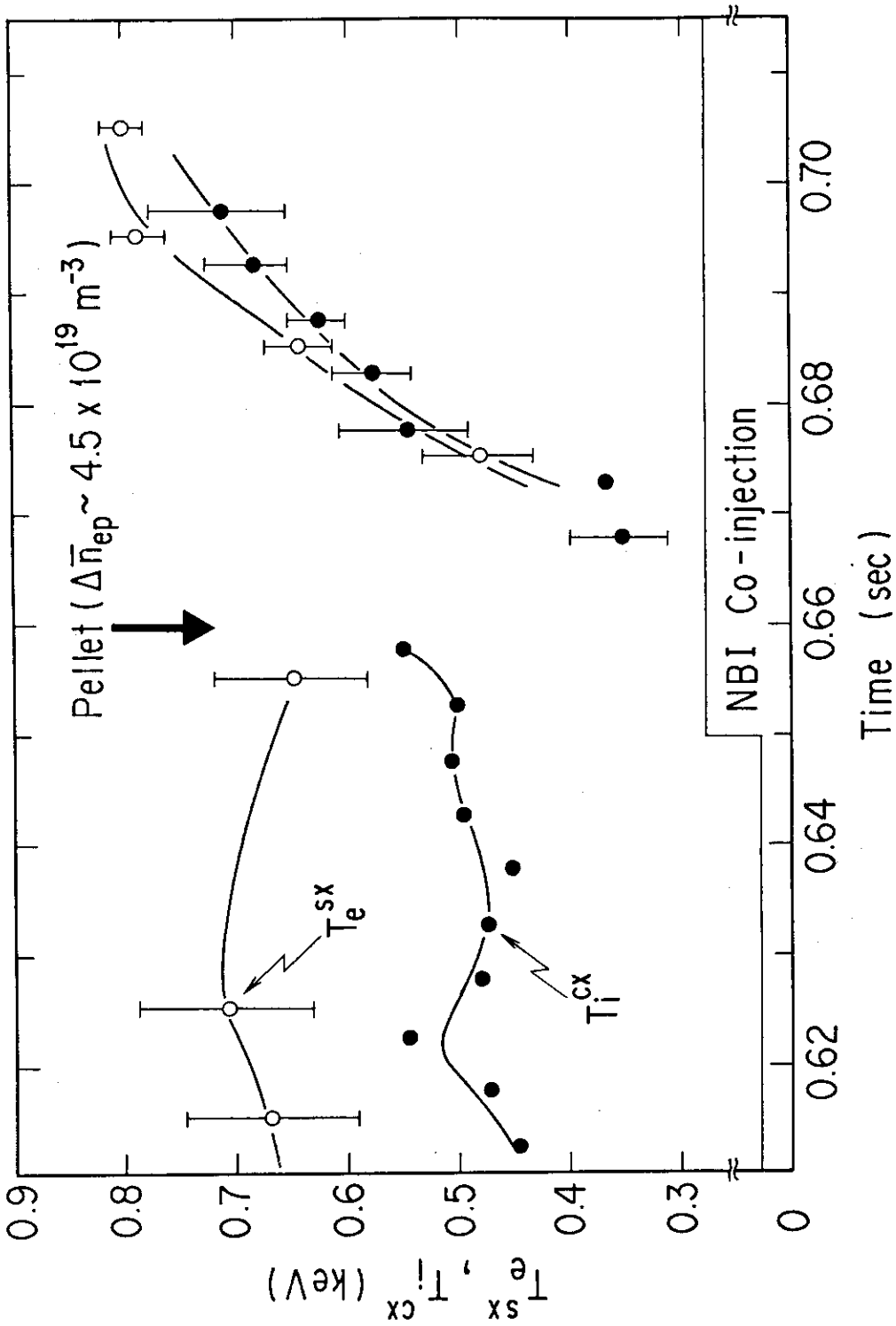

Fig. 7 Time evolution of central electron and ion temperature of type 2 discharge measured by soft X-ray and mass-separated neutral particle measurement.

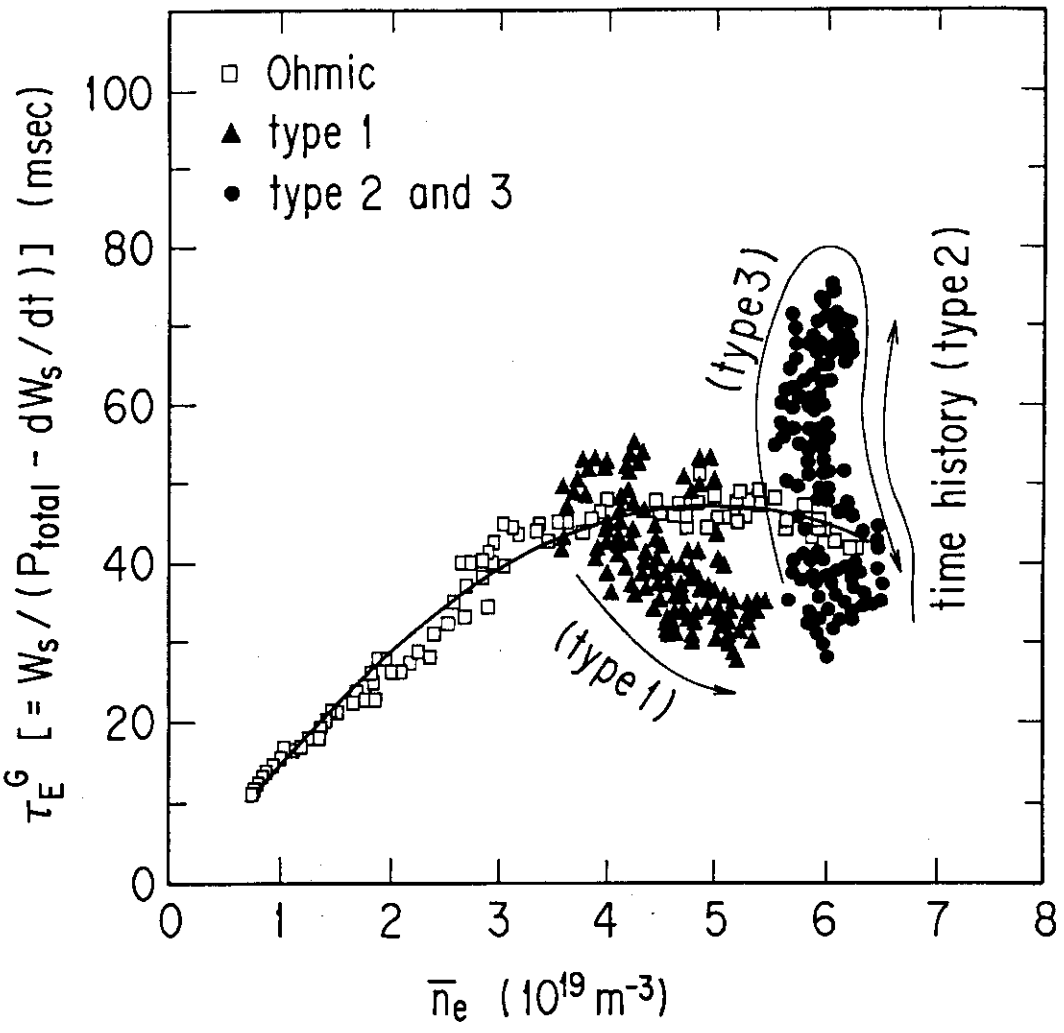

Fig. 8 Line-averaged electron density ($\bar{n}_e$) versus global energy confinement time (τ_E^G). Squares (□) are τ_E^G of ohmically heated discharges, closed triangles (▲) are τ_E^G of type 1 discharges, closed circles (●) are τ_E^G of type 2 and type 3 discharges. Arrows show the time history of τ_E^G in type 1, 2 and 3 discharges.

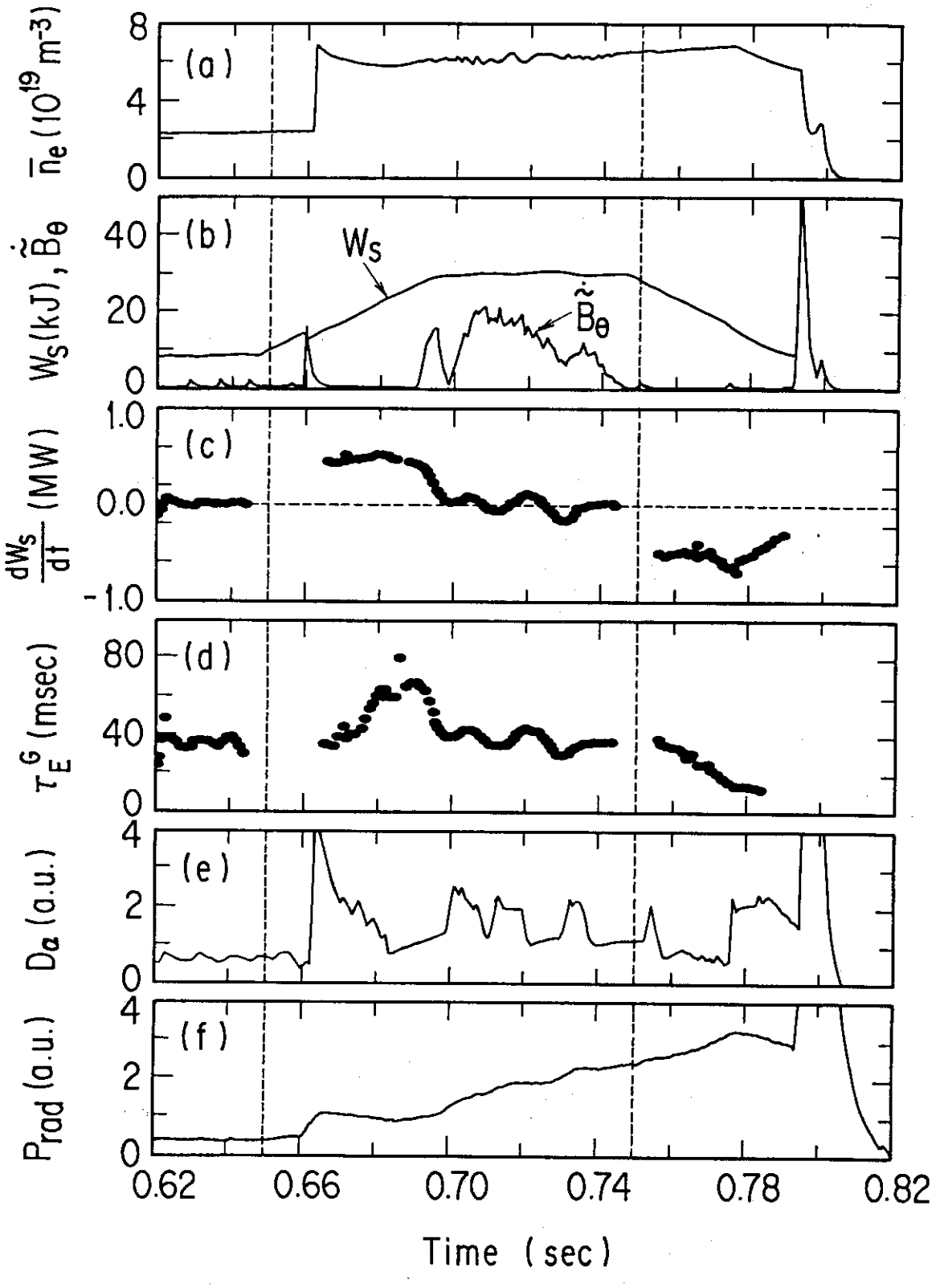

Fig. 9 Time evolution of various plasma parameters of type 3: columns from (a) to (f) are the same as Fig. 4(a) to Fig. 4(f), respectively.

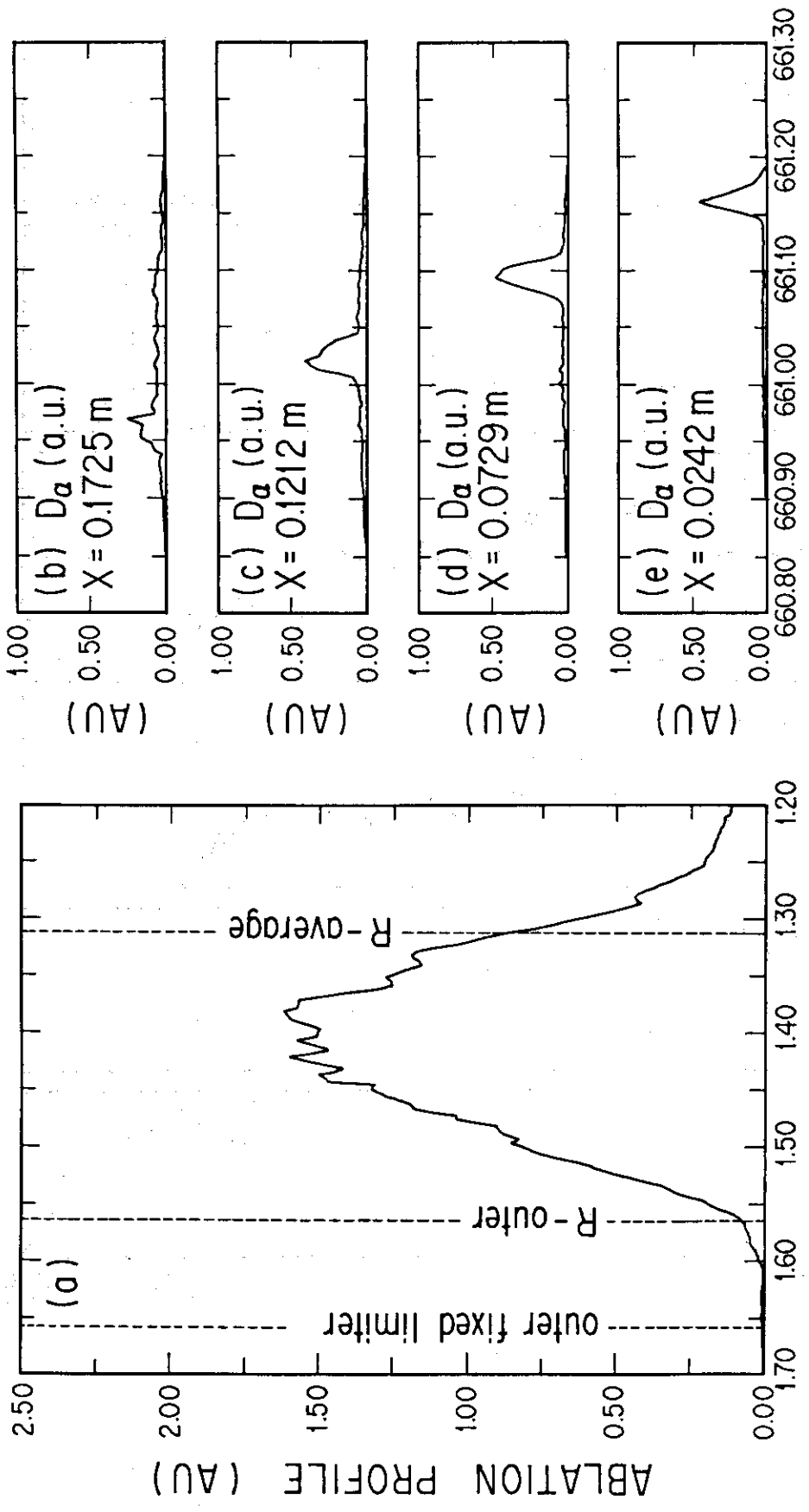

Fig. 10 Ablation profiles of the pellet of type 3 discharge: columns from (a) to (e) are the same as Fig. 6(a) to Fig. 6(e), respectively.